

## Supporting Information

to

### **Stabilization of alkaline 5-HMF electrolytes via Cannizzaro reaction for the electrochemical oxidation to FDCA**

Moritz Lukas Krebs<sup>a</sup>, Alexander Bodach<sup>a</sup>, Changlong Wang<sup>b,\*</sup>, Ferdi Schüth<sup>a,\*</sup>

<sup>a</sup>*Department of Heterogeneous Catalysis, Max-Planck-Institut für Kohlenforschung, Kaiser-Wilhelm-Platz 1, 45470 Mülheim an der Ruhr, Germany*

<sup>b</sup>*Institute of Circular Economy, Faculty of Materials and Manufacturing, Beijing University of Technology, Beijing 100124, PR China*

\*Corresponding Authors

Ferdi Schüth (E-mail: [schueth@kofo.mpg.de](mailto:schueth@kofo.mpg.de))

Changlong Wang (E-Mail: [changlongwang1987@gmail.com](mailto:changlongwang1987@gmail.com))

## Table of Contents

1. General .....	3
2. Experimental Procedures .....	3
2.1. Catalyst preparation .....	3
2.2. Characterization .....	3
2.3. Electrochemical measurements .....	3
2.4. HPLC measurements .....	4
2.5. Quantitative NMR measurements .....	4
2.6. HMF degradation tests .....	5
3. NMR measurements .....	6
3.1. Stability assessment of the electrolyte .....	6
3.2. Exemplary qNMR measurements .....	8
3.3. HMF in 1 M KOH .....	11
3.4. DHMF in 1 M KOH .....	12
3.5. HMFCA in 1 M KOH .....	13
3.6. FDCA in 1 M KOH .....	14
4. Electrochemical experiments .....	15
4.1. Electrochemical HMF oxidation .....	15
4.2. Electrochemical oxidation of the Cannizzaro products .....	18
5. HPLC measurements .....	20
5.1. HPLC traces at 270 nm .....	20
5.2. Exemplary HPLC measurement .....	21
6. Catalyst characterization .....	23
7. Testing of indirect HMF oxidation for other catalytic systems .....	24
7.1. Unmodified Ni-Foam .....	24
7.2. Mesoporous $\text{Co}_3\text{O}_4$ .....	25
7.3. Pt-foil .....	27
8. References .....	29

## 1. General

All solvents and chemicals were used as purchased without further purifications. Chemicals: 5-hydroxymethylfurfural (5-HMF; stored at 3 °C, Sigma-Aldrich, 99%), 2,5-furandicarboxylic acid (FDCA; AlfaAesar, 98%), diformylfuran (DFF; Sigma-Aldrich, 97%), 5-hydroxymethyl-2-furancarboxylic acid (HMFCA; BLDpharm, 99%), 5-formyl-2-furancarboxylic acid (FFCA; TCI, 98%), dihydroxymethylfuran (DHMF; BLDpharm, 98%), iron(III) chloride hexahydrate (reagent grade, ≥ 98%, Sigma-Aldrich), cobalt nitrate hexahydrate (Sigma-Aldrich, ACS reagent, 98%), 35 wt.% H<sub>2</sub>O<sub>2</sub> (J. T. Baker), Nafion™ 117 (Sigma-Aldrich), potassium hydroxide (KOH, reagent pellet; VWR Chemicals ≥ 85%), Ni foam (Recemat BV, Netherlands), Carbon paper (Toray Carbon paper, TGP-H-60, Alfa Aesar), and perfluorinated membrane made from Nafion™ 117 (Sigma-Aldrich).

Prior to the synthesis, all the flasks were washed with HCl to remove any traces of metal residue. This was followed by washing with water and acetone and a final drying step at 80 °C overnight. Milli-Q water (18.2 MΩ) was used for all the syntheses and catalysis experiments.

## 2. Experimental Procedures

### 2.1. Catalyst preparation

Prior to Fe-modification, nickel foams (NF) were cut into slices (1 cm x 3 cm) and were then cleaned by ultrasonication sequentially using hydrochloric acid (3 M), acetone, ethanol, and ultrapure water for 15 min, respectively. The cleaned NF was immediately put into a 50 mL beaker containing a mixture of FeCl<sub>3</sub>·6H<sub>2</sub>O (2.5 mmol) and 5% H<sub>2</sub>O<sub>2</sub> (25 mL) that had been reacted for 5 mins. After 1 min of treatment, the solution was decanted and rinsed with MQ water. Finally, the modified foam was put into a plastic petri dish and dried at 60 °C in an oven for 24 h.

### 2.2. Characterization

**Scanning electron microscopy (SEM):** Images were taken with a Hitachi TM3030 microscope. The EDX analyses were performed with an SDD detector and software from Oxford instruments.

**Inductively coupled plasma-optical emission spectrometry (ICP-OES):** Measurements were carried out on a Spectro Green FMX 46 ICP-OES. To dissolve the Ni-foams, aqua regia at elevated temperatures was used. The solution was subsequently diluted with MQ water and then measured. The resulting signals were quantified by a multi-element standard obtained from Bernd Kraft.

### 2.3. Electrochemical measurements

Electrochemical measurements were performed using a Gamry Interface 1010 B electrochemical workstation at room temperature with a three-electrode system in an H-type cell, separated by a Nafion 117 membrane. A coiled Pt-wire was used as the counter electrode (CE), the Hg/HgO electrode as the reference electrode (RE), and the Ni-foam (~1 cm x 1 cm) as the working electrode (WE). All reactions were performed in 5 mL of the corresponding electrolyte. Organic substrates were added only into the anode compartment. Stirring was applied for both the anode and cathode chamber at 250 rpm in the cathode and 500 rpm in the anode chamber. In a typical electrochemical experiment sequence, cyclic voltammetry (CVs) at a rate of 100 mV/s from 0.00 – 0.70 V vs. Hg/HgO for 20 cycles were measured to guarantee a stable electrode performance during the experiments. Linear sweep voltammetry (LSV) with a scan rate of 5 mV s<sup>-1</sup> was then used to evaluate the performance of the electrode in an electrochemical reaction. The potential between the WE and RE is given as the measured potential versus the used Hg/HgO reference electrode. The measured potentials during the LSV measurements are corrected by the uncompensated solution resistance  $R_s$

$$E(\text{Hg/HgO} - \text{corrected}) = E(\text{Hg/HgO}) - j \cdot R_s \quad (1)$$

where  $j$  are the measured currents. To determine  $R_s$ , electrochemical impedance spectroscopy (EIS) at 0.30 V vs. Hg/HgO was performed and  $R_s$  was then extracted from the high-frequency regime. This

measurement was repeated three times to average measurement errors. Constant potential electrolysis was typically performed at 0.50 V vs. Hg/HgO with a total electrolyte volume of 5 mL for each chamber. Generally, the potentials can be converted referencing the reversible hydrogen electrode (RHE) through the Nernst equation (2)

$$E(\text{RHE}) = E(\text{Hg}/\text{HgO}) + 0.059 \cdot \text{pH} - 0.118\text{V} \quad (2)$$

where 0.118 V is the standard potential of the Hg/HgO reference electrode at 25°C versus an RHE reference electrode (as given by the supplier ALS). However, typically a standard potential of 0.098 V is used in the literature.<sup>1</sup>  $E(\text{Hg}/\text{HgO})$  is the potential measured in the experiment and pH denotes the pH value of the electrolyte – which, however, needs to be calculated using activities for the solution conditions. We also measured the potential of the Hg/HgO electrode. The measured potential versus an RHE reference electrode was 0.928 V in 1M KOH and 0.950 V in 5M KOH. Since the different published potentials of Hg/HgO, the potential given by the manufacturer, and our own referencing for converting potentials to RHE are not fully consistent, we decided to give all potentials as measured with the Hg/HgO electrode, only corrected for the uncompensated solution resistance.

## 2.4. HPLC measurements

HPLC was used to analyze the products of HMF oxidation quantitatively and calculate the corresponding Faradaic efficiencies (FE). To do this, electrolyte samples were taken from the cell and analyzed by HPLC. The HPLC system consists of a Shimadzu LC-2030 chromatograph equipped with a 100 mm organic acid resin column with 8.0 mm inner diameter and a pre-column (40 mm organic acid resin with 8.0 mm i.d.). As the mobile phase, a 2 mM aqueous solution of trifluoroacetic acid was used with a flow rate of 1 mL min<sup>-1</sup> at a temperature of 40 °C. For the detection of the organic substrates, a UV detector (270 nm) was used and external one-point calibration was applied to quantify HMF, HMFCa, DFF, FFCA, furoic acid, and FDCA. The conversion of the substrates (%) and the yields (%) of FDCA were calculated using equations (3) and (4)

$$\text{substrate conversion (\%)} = [n(\text{substrate consumed}) / n(\text{substrate initial})] \cdot 100\% \quad (3)$$

$$\text{product yield (\%)} = [n(\text{product}) / n(\text{initial substrate})] \cdot 100\% \quad (4)$$

FE were calculated according to equation (5)

$$\text{FE (\%)} = [n(\text{FDCA formed}) / (\text{charge} / (N(e^-) \times F))] \cdot 100\% \quad (5)$$

with  $N(e^-)$  representing the number of transferred electrons needed to oxidize the corresponding substrate to FDCA (e.g.  $N(e^-) = 6$  for HMF oxidation). To determine the FE of FDCA production when a mixture of the Cannizzaro products is oxidized, we assume an average oxidation of 6 e<sup>-</sup> based on the 8 e<sup>-</sup> oxidation for DHMF to FDCA and 4 e<sup>-</sup> oxidation for HMFCa to FDCA. This is justified since conversions of ~95 % are achieved while confirming that both educts are oxidized at the same time.

## 2.5. Quantitative NMR measurements

NMR spectra were recorded with a Bruker 300 MHz AVIIIHD nanobay NMR spectrometer. Generally, spectra were measured at 300 K. <sup>1</sup>H chemical shifts are reported relative to DSS using DMSO as internal reference as described by Babij *et al.*<sup>2</sup> All chemical shifts ( $\delta$ ) are reported in ppm, coupling constants are given in Hz, and common abbreviations are used. Quantitative data from reaction mixtures were extracted from <sup>1</sup>H-NMR spectra (spectral width = 20 ppm) with perfect echo excitation sculpting for water suppression prior to acquisition (Bruker pulsesequence: zgesgppe).<sup>3,4</sup> Generally, 8 FIDs containing 65536 complex datapoints were averaged and a relaxation delay of 70 s between individual scans was used to ensure full relaxation of the individual components. Prior to acquisition, the chemical shift of the water signal was automatically determined with an AU program (modified version of Bruker version: au\_watersc with a shorter relaxation delay of 1 s) which was then used as central offset for the measurement (O1) to ensure optimal water suppression. Although the selective pulse used in the sequence might lead to suppression of other signals as well, the quantitative outcomes for the signals of interest were validated with reference samples (see Figure S6 – S9).

The concentration of the substance was determined according to equation (6)

$$c(\text{substrate}) = c(\text{DMSO}) \cdot [I(\text{substrate}) \cdot 6H] / [I(\text{DMSO}) \cdot N(\text{proton substrate})] \quad (6)$$

$I$  being the measured integral and  $N(\text{proton})$  the number of protons connected to the signal. To prevent H/D-exchange reactions in strongly alkaline media, a capillary filled with  $D_2O$  was used for locking and shimming. To slow down the decomposition reactions, the electrolyte was diluted with MQ water. Since the signals of hydrogen atoms with  $^1H$  chemical shifts close to the water signal are affected by the suppression sequence, we do not label or integrate those signals since this might result in a misleading interpretation of the data.

## 2.6. HMF degradation tests

The degradation experiments of HMF were typically performed in glass vial by adding 2 mL of KOH solution and the desired amount of HMF. The solution was then stirred at 400 rpm at room temperature. To measure decomposition at lower temperatures ( $0\text{ }^\circ\text{C}$ ), 10 mL of cooled KOH solution ( $0\text{ }^\circ\text{C}$ ) were added to the desired amount of HMF into a 50 mL flask and then stirred in an ice bath at 400 rpm. Reaction products were quantified after 20 h using qNMR measurements by adding a known amount of DMSO as an internal standard.

### 3. NMR measurements

#### 3.1. Stability assessment of the electrolyte

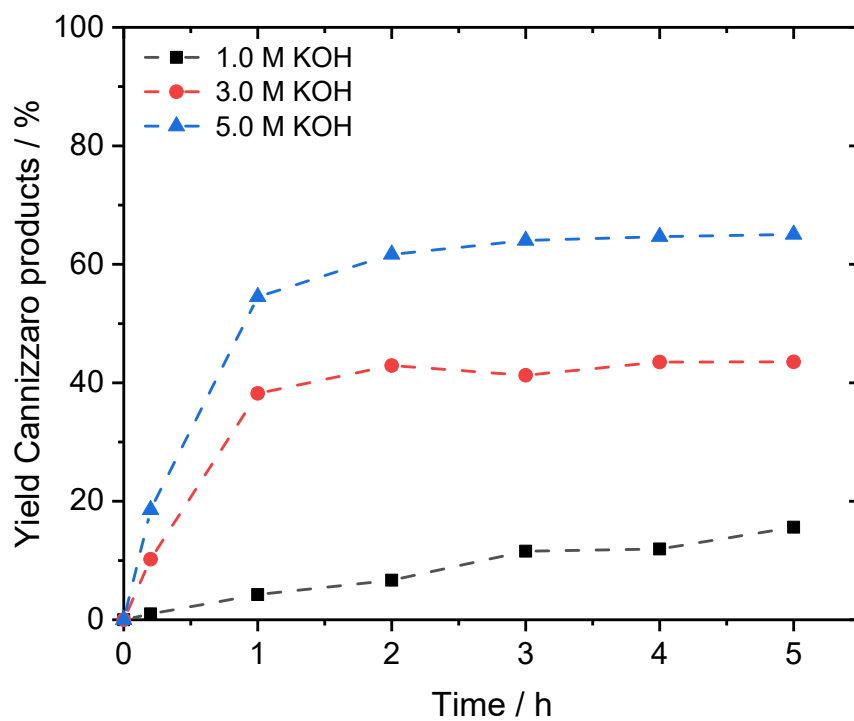


**Figure S1:** Cannizzaro product formation (DHMF and HMFA) when HMF is stirred in 1.0 M KOH (black squares), 3.0 M KOH (red circles), and 5.0 M KOH (blue triangles) at room temperature under ambient pressure. The concentration of HMF was kept at 0.05 M for all prepared solutions. Solutions were stirred and quantification was performed via qNMR. 100% is based on the initial mass of HMF. Dashed lines are used as a guide to the eyes.

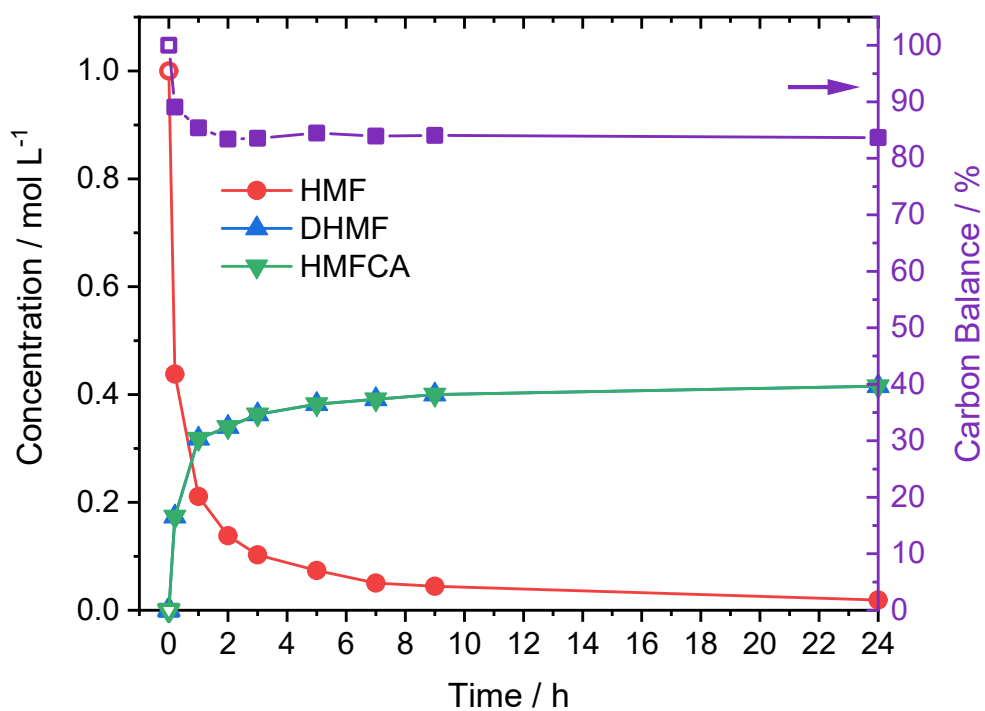


**Figure S2:** Time resolved transformation of a 1.0 M HMF solution in a 5 M KOH solution at 0 °C under ambient pressure. Quantification was performed using qNMR with DMSO as an internal standard. 100% is based on the initial mass of HMF and assumed to be the starting point (unfilled symbols). Concentrations of DHMF and HMFCAs are almost equal and symbols are thus superimposed and difficult to distinguish.

### 3.2. Exemplary qNMR measurements

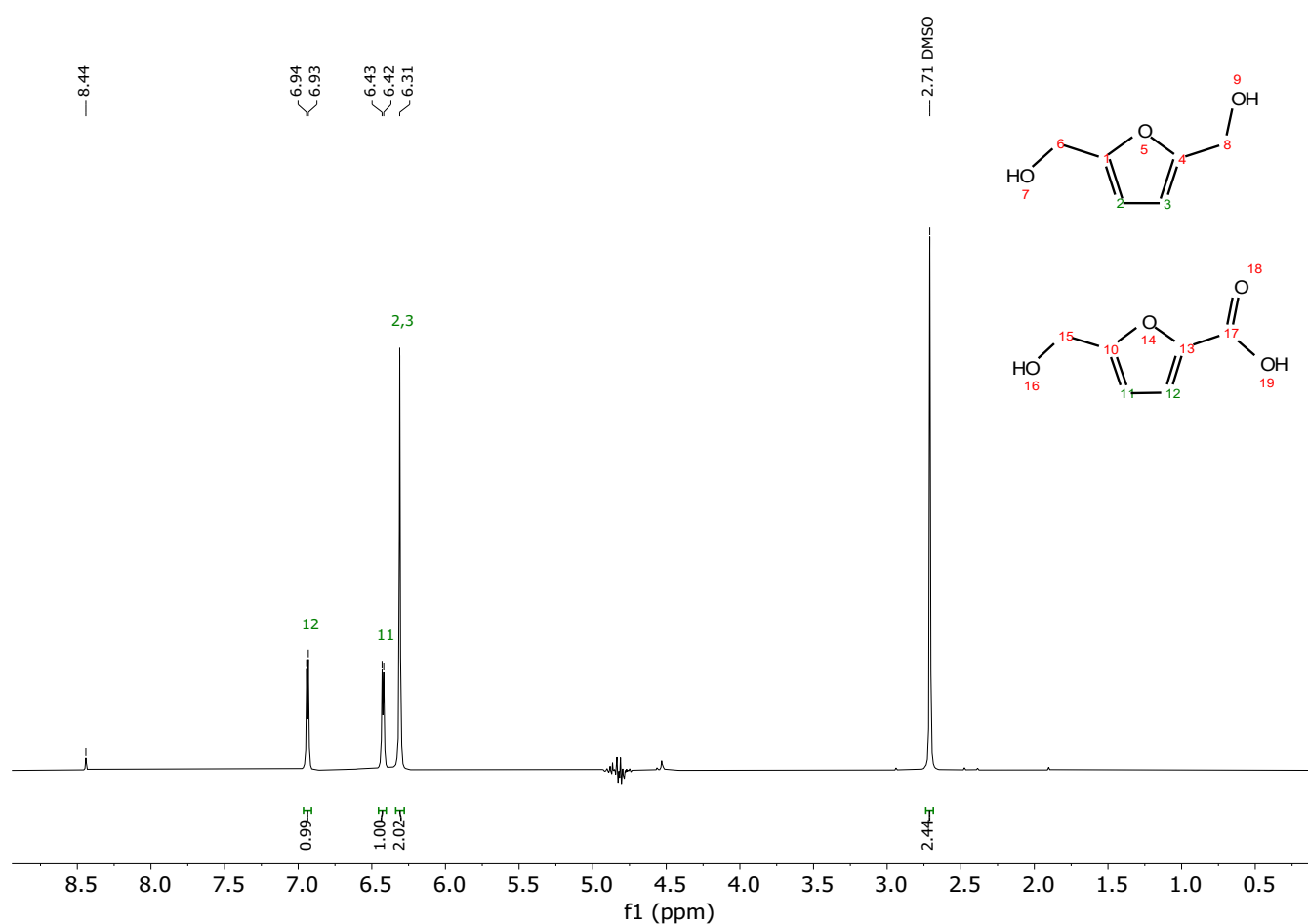


**Figure S3:** Exemplary qNMR spectrum with water suppression of a HMF solution after transformation in 5 M KOH (H<sub>2</sub>O). Unlabeled hydrogen atoms (6, 8, and 15) are neglected for analysis since they are affected by the water suppression measurement sequence. The sample was diluted with MQ water before the qNMR measurement. Chemical shifts are referenced by the DMSO signal.<sup>2</sup>

HMFCFA: <sup>1</sup>H NMR (300 MHz, H<sub>2</sub>O/KOH) δ/ppm = 6.94 (d, *J* = 3.4 Hz, 1H), 6.42 (d, *J* = 3.4 Hz, 1H).  
DHMF: <sup>1</sup>H NMR (300 MHz, H<sub>2</sub>O/KOH) δ/ppm = 6.31 (s, 2H).

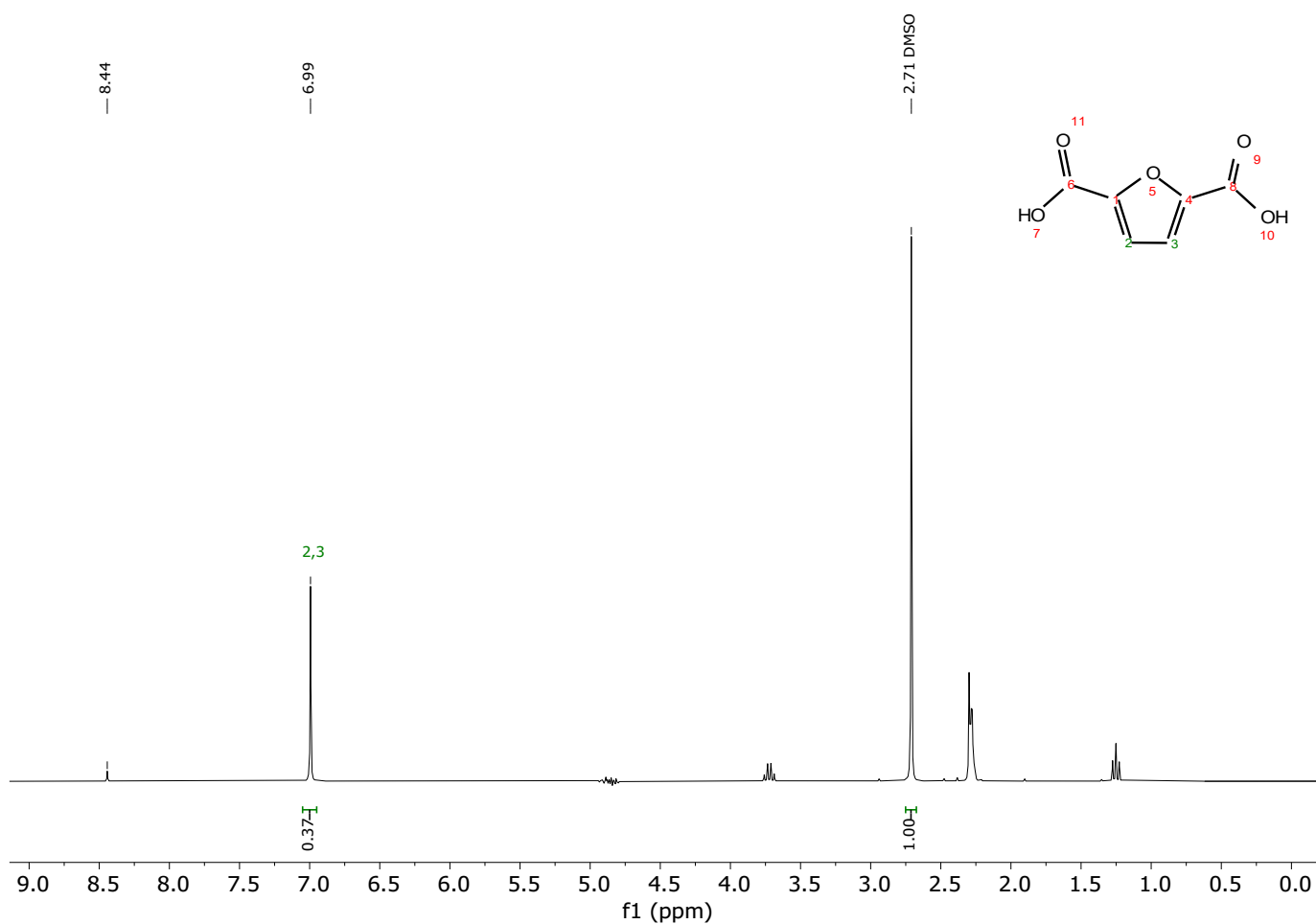


**Figure S4:** Exemplary qNMR after electrolysis of HMFCa and DHMF (0.05 M, 1M KOH), demonstrating conversion to FDCA. The sample was diluted with MQ water before the qNMR measurement. Unlabeled hydrogen atoms are affected by the water suppression measurement sequence. Signals at ~ 3.7 ppm and ~ 1.3 ppm are artifacts of the measurement sequence and do not have any analytical relevance. Chemical shifts are referenced by the DMSO signal.<sup>2</sup>

FDCA:  $^1\text{H}$  NMR (300 MHz,  $\text{H}_2\text{O}/\text{KOH}$ )  $\delta/\text{ppm} = 6.99$  (s, 2H).

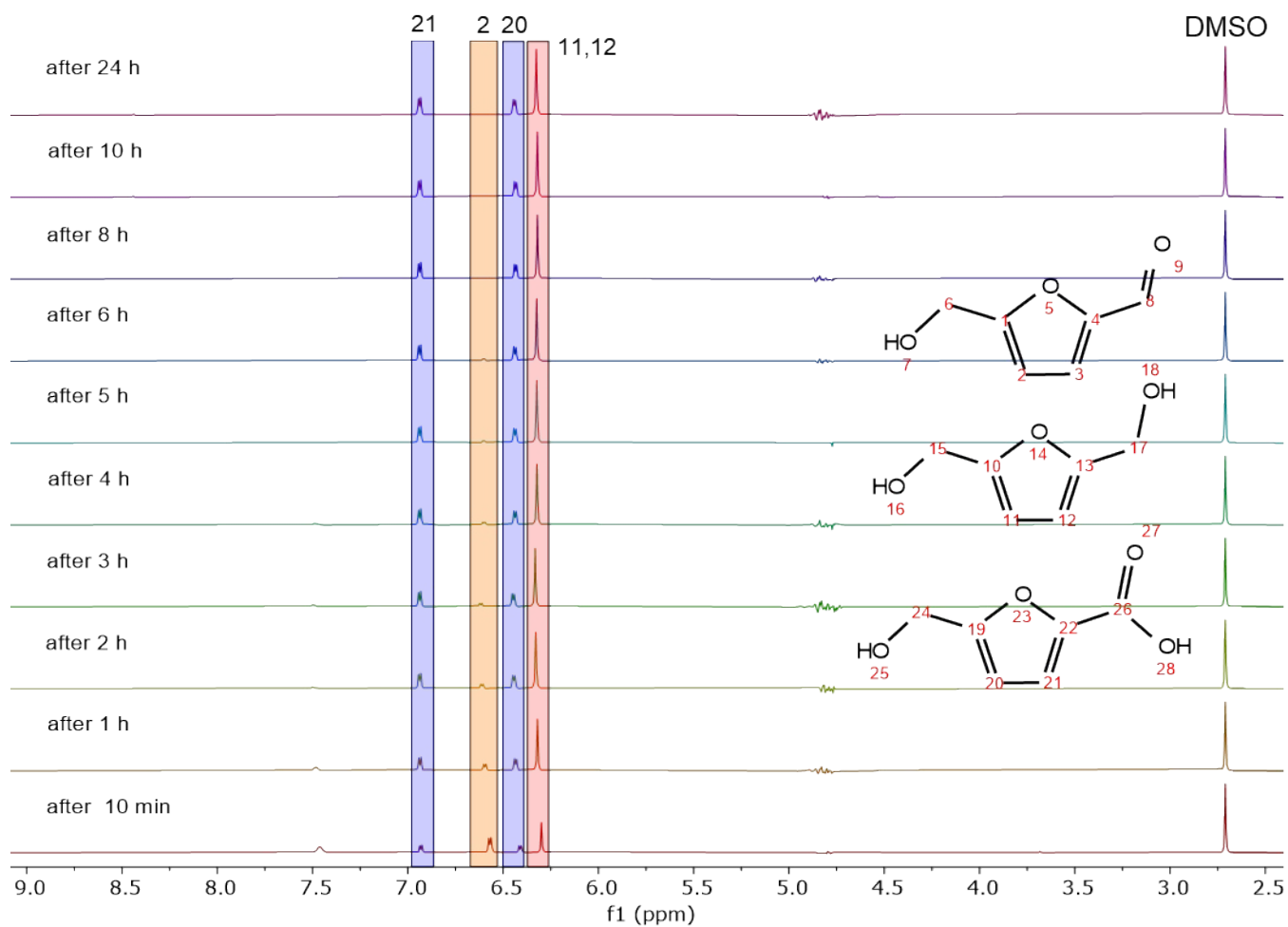


**Figure S5:** Time resolved transformation of HMF into HMFA and DHMF in 5 M KOH at 0 °C. Samples were diluted with MQ water before NMR measurement. Chemical shifts are referenced by using DMSO as an internal standard. Assignment of the signals according to the identifiers: HMF (orange), HMFA (blue), and DHMF (red).

### 3.3. HMF in 1 M KOH

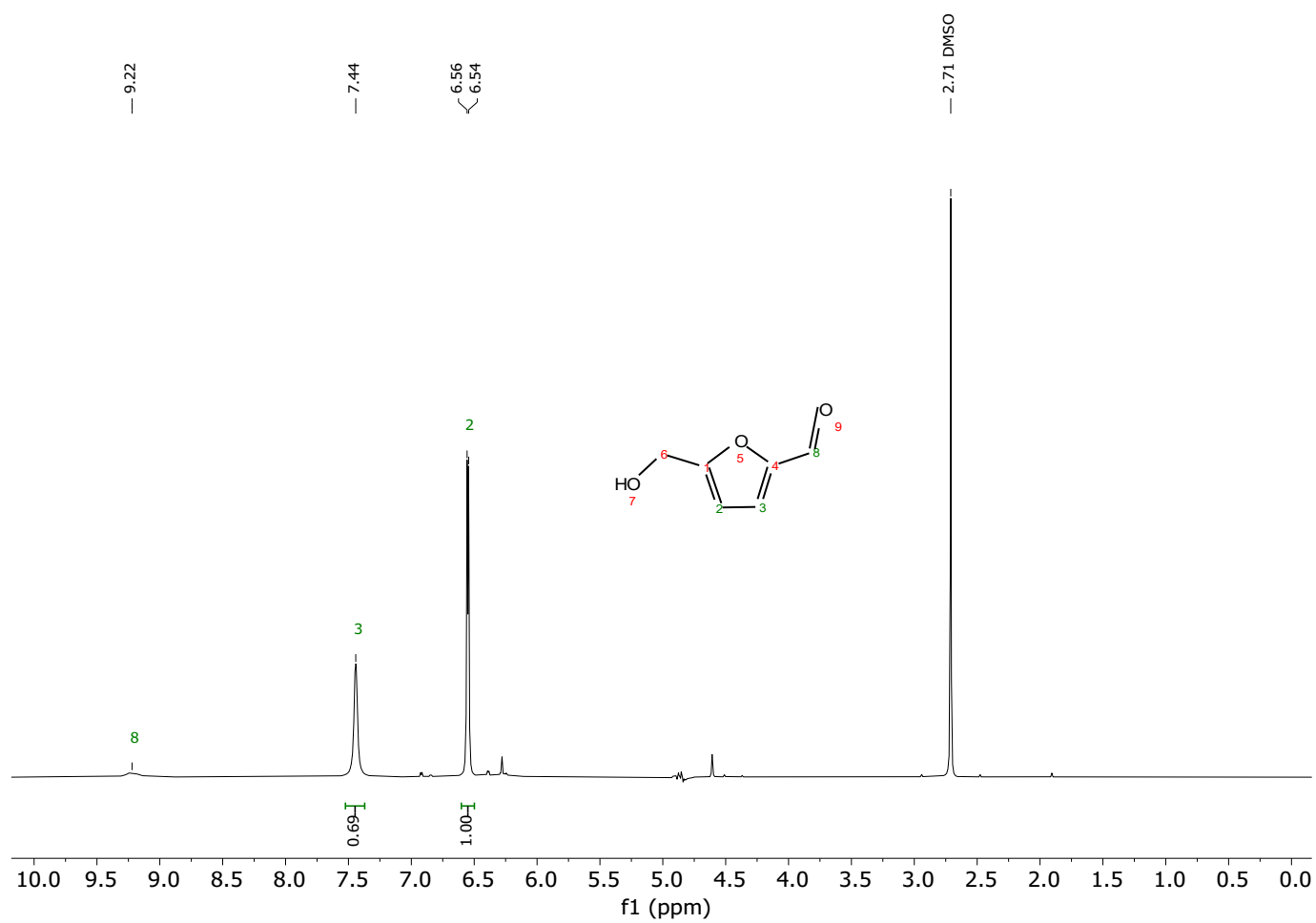


**Figure S6:** NMR spectra of commercial HMF in an aqueous 1 M KOH. Chemical shifts are referenced by the DMSO signal.<sup>2</sup>

HMF: <sup>1</sup>H NMR (300 MHz, 1 M KOH)  $\delta$ /ppm = 9.22 (s, 1H), 7.44 (s, 1H), 6.55 (d, J = 3.7 Hz, 1H).

### 3.4. DHMF in 1 M KOH

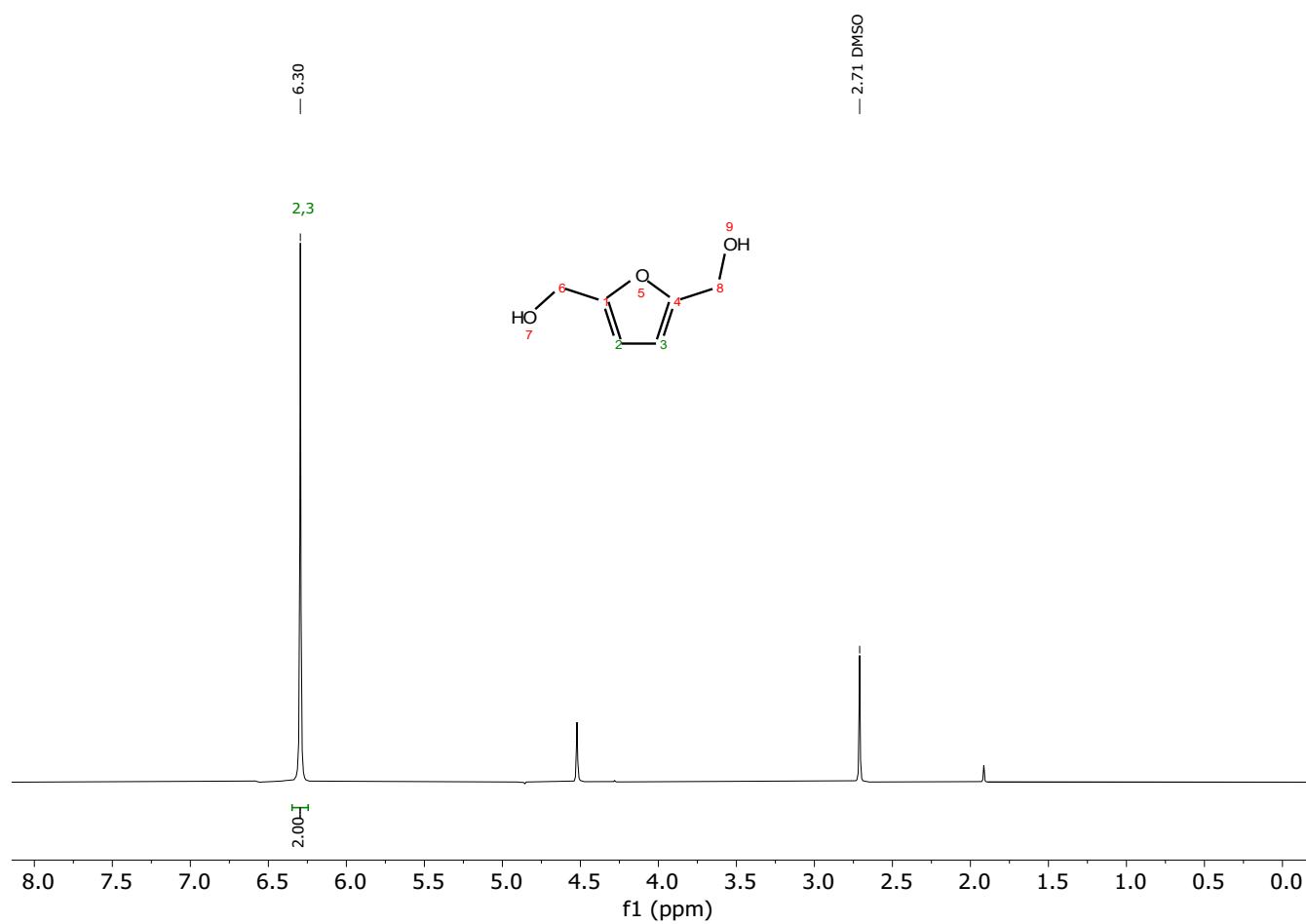


**Figure S7:** NMR spectra of commercial DHMF in an aqueous 1 M KOH. Chemical shifts are referenced by the DMSO signal.<sup>2</sup>

DHMF: <sup>1</sup>H NMR (300 MHz, 1 M KOH)  $\delta$ /ppm = 6.30 (s, 2H).

### 3.5. HMFCA in 1 M KOH

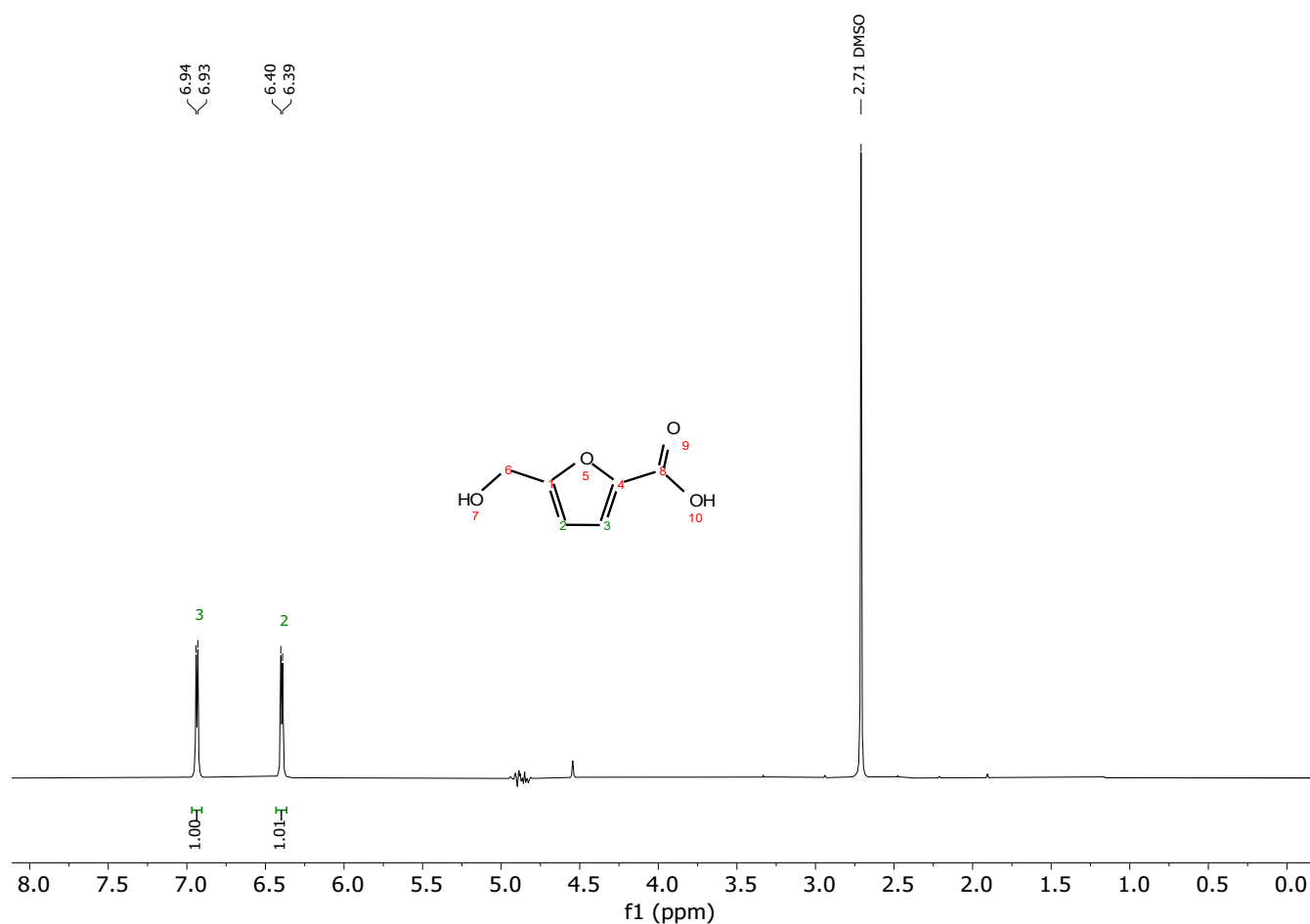


**Figure S8:** NMR spectra of commercial HMFCA in an aqueous 1 M KOH. Chemical shifts are referenced by the DMSO signal.<sup>2</sup>

HMFCA: <sup>1</sup>H NMR (300 MHz, 1 M KOH)  $\delta$ /ppm = 6.94 (d,  $J$  = 3.4 Hz, 1H), 6.40 (d,  $J$  = 3.4 Hz, 1H).

### 3.6. FDCA in 1 M KOH

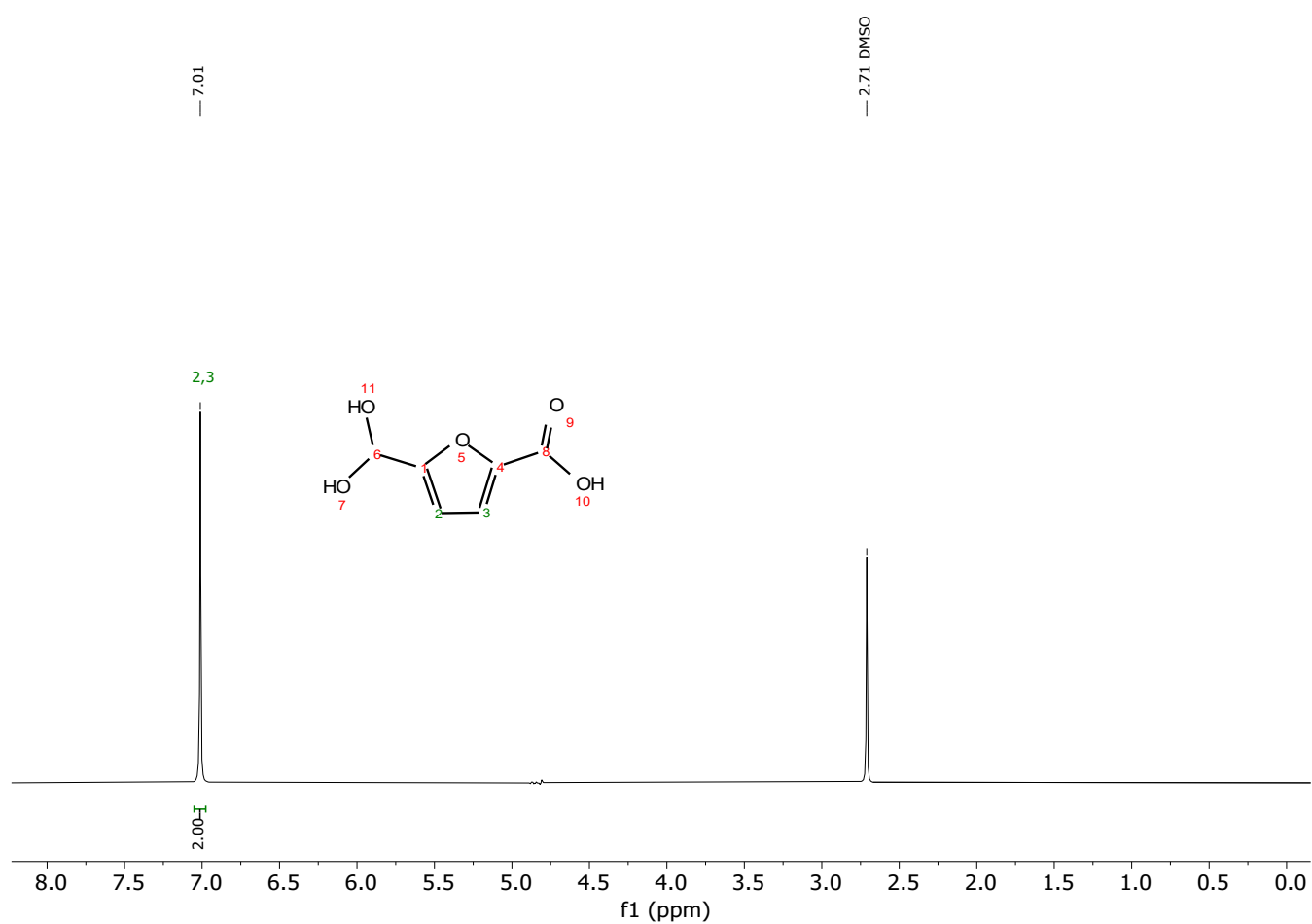


**Figure S9:** NMR spectra of commercial FDCA in an aqueous 1 M KOH. Chemical shifts are referenced by the DMSO signal.<sup>2</sup>

FDCA:  $^1\text{H}$  NMR (300 MHz, 1 M KOH)  $\delta/\text{ppm} = 7.01$  (s, 2H).

## 4. Electrochemical experiments

### 4.1. Electrochemical HMF oxidation

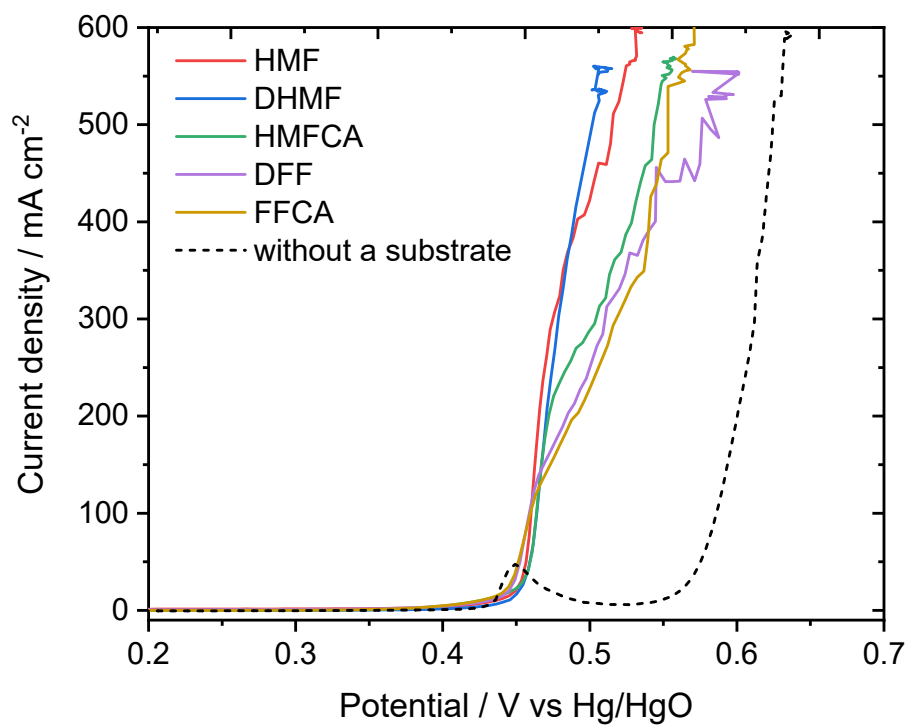


**Figure S10:** LSV curves of Fe-modified Ni-foams in the oxidation of different organic substrates (each 0.05 M) in 1 M KOH with a scan rate of 5 mV s<sup>-1</sup>. Potentials are corrected for the uncompensated solution resistance.

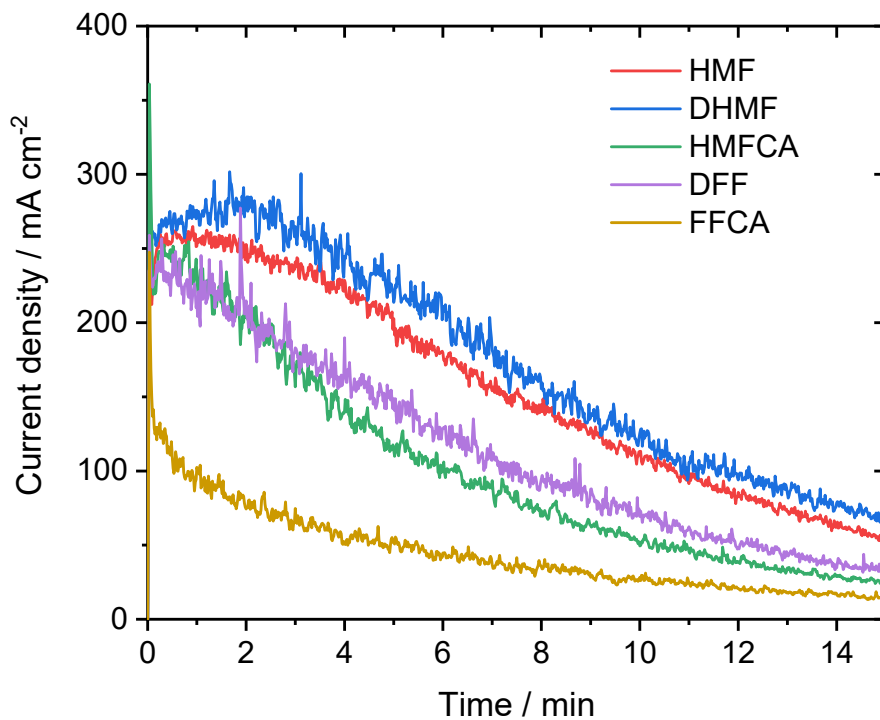


Figure S11: Constant potential electrolysis (0.50 V vs. Hg/HgO) in 1 M KOH, including 50 mM of different organic substrates.

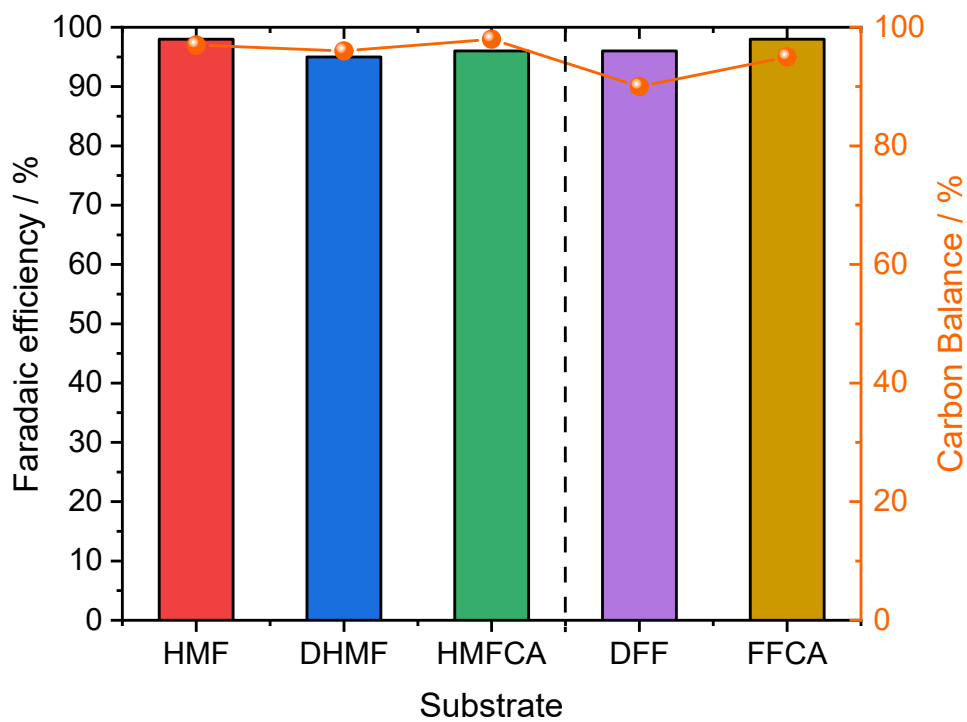
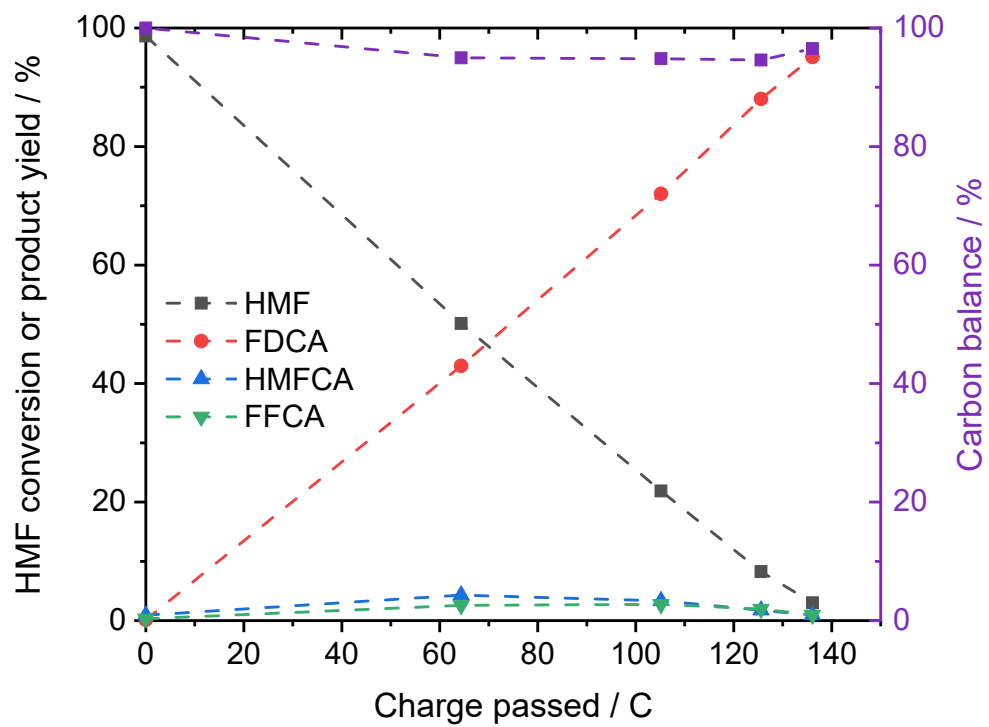
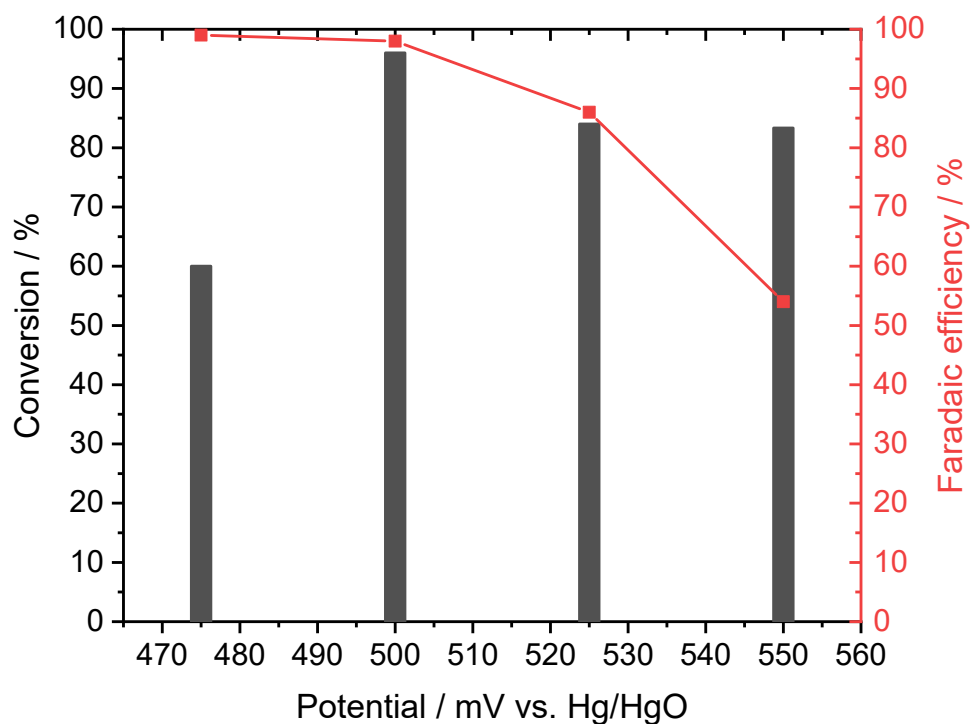


Figure S12: Faradaic efficiency and carbon balance for different substrates and intermediates of the HMF oxidation to FDCA after constant potential electrolysis (0.50 V vs. Hg/HgO) for 15 min.



**Figure S13:** Time resolved product formation in the alkaline oxidation of a 0.05 M HMF solution in the presence of 1 M KOH during constant potential electrolysis (0.50 V vs. Hg/HgO) for 15 min.

## 4.2. Electrochemical oxidation of the Cannizzaro products



**Figure S14:** Conversions and FE for the oxidation of the Cannizzaro products (0.05 M based on initial HMF concentration) after constant potential electrolysis at different potentials for 15 min, utilizing the Fe-modified Ni-foams as the working electrode.

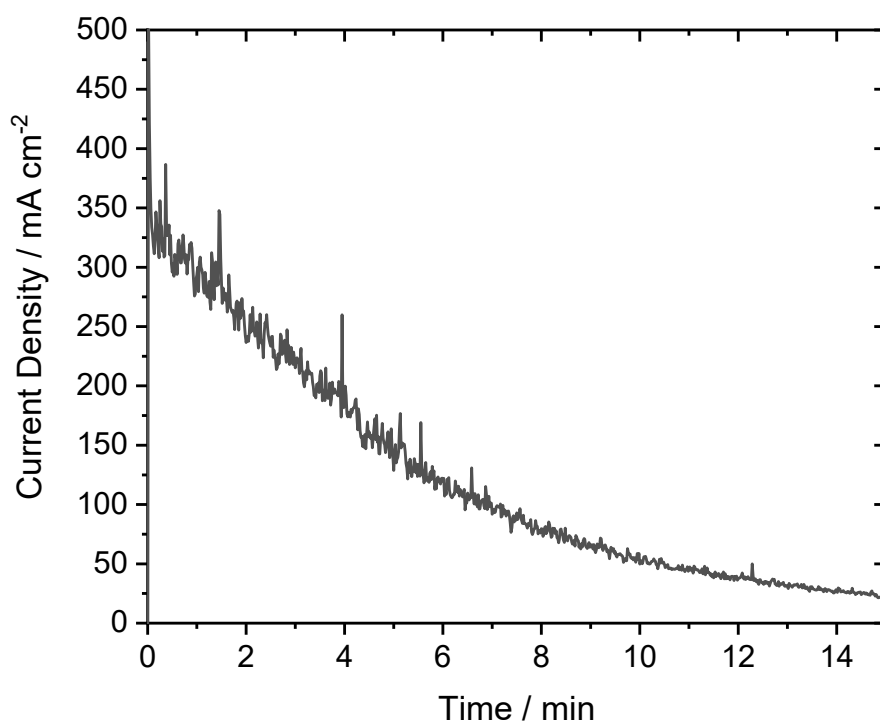


**Figure S15:** Constant potential electrolysis (0.50 V vs. Hg/HgO) in 1 M KOH including 0.05 M of the Cannizzaro products (DHMF and HMFC; based on initial HMF input before degradation).

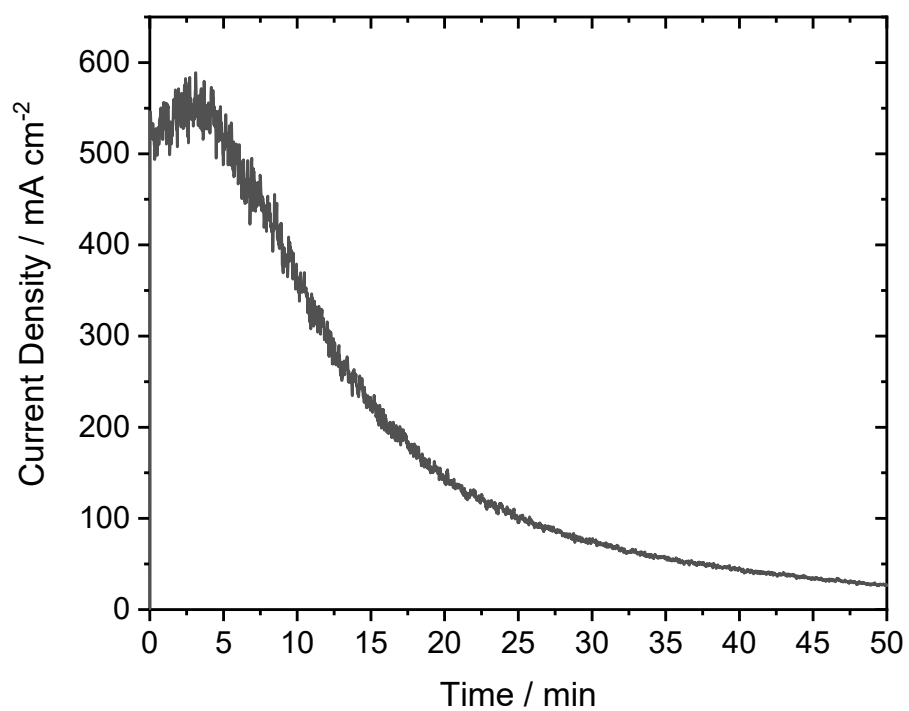


**Figure S16:** Constant potential electrolysis (0.47 V vs. Hg/HgO) in 5M KOH, including 0.25 M of the Cannizzaro products (DHMF and HMFA; based on initial HMF input before degradation). Even higher current densities were achieved at higher potentials (Figure 3a) but were not accessible for a 1 cm x 1 cm electrode do to technical limitations of the potentiostat.

## 5. HPLC measurements

### 5.1. HPLC traces at 270 nm

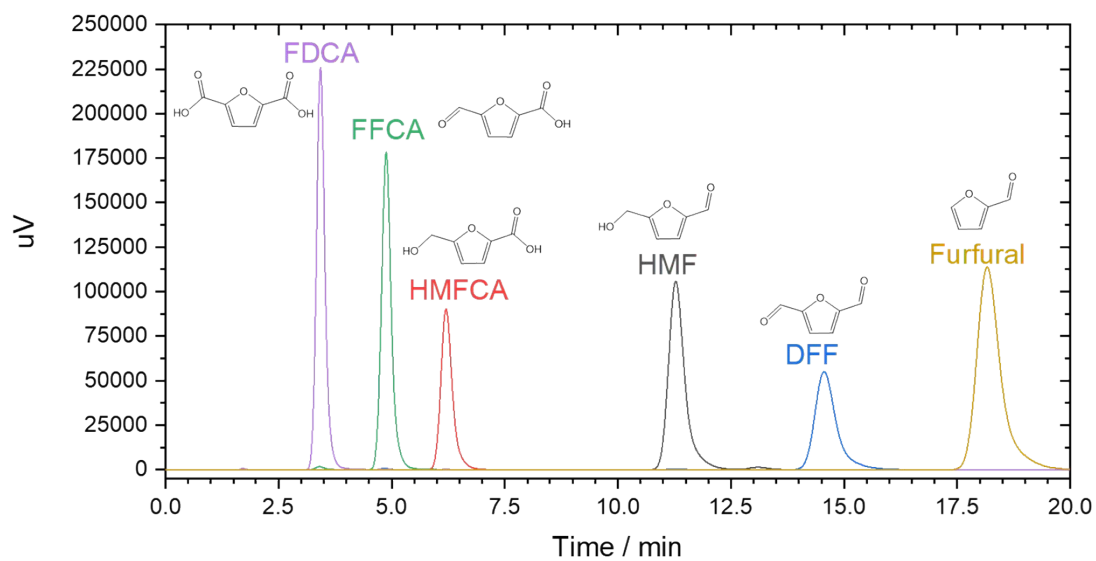


**Figure S17:** HPLC traces obtained for potential reaction intermediates and products in the HMF oxidation. All traces were measured independently as pure substances in H<sub>2</sub>O (1 mg/mL) and detected via UV detector (270 nm).

## 5.2. Exemplary HPLC measurement

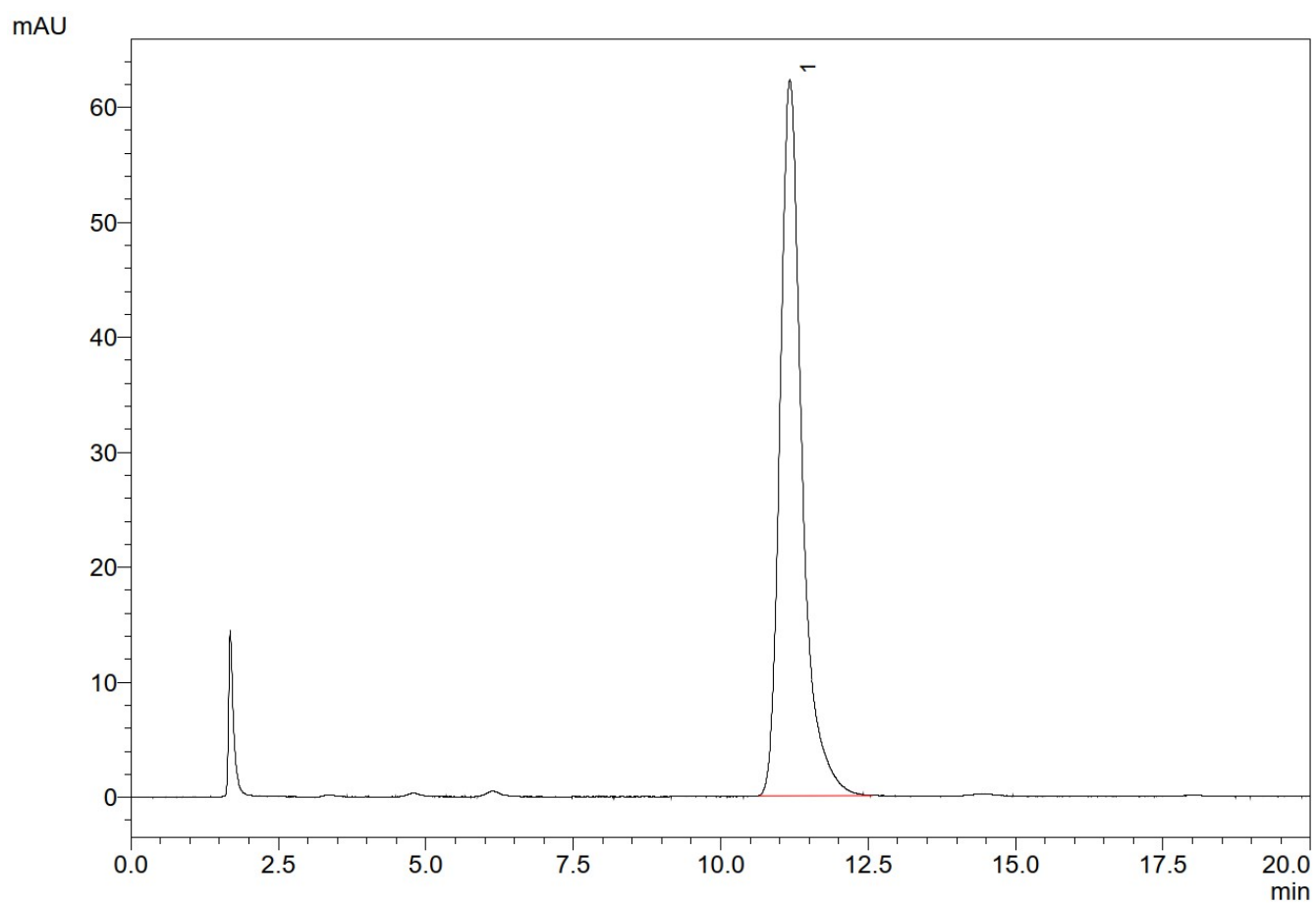


**Figure S18:** HPLC measurement of an electrolyte containing 50 mM HMF in 1 M KOH before the electrochemical transformation. Assignment of the signals according to the identifiers: HMF (1).

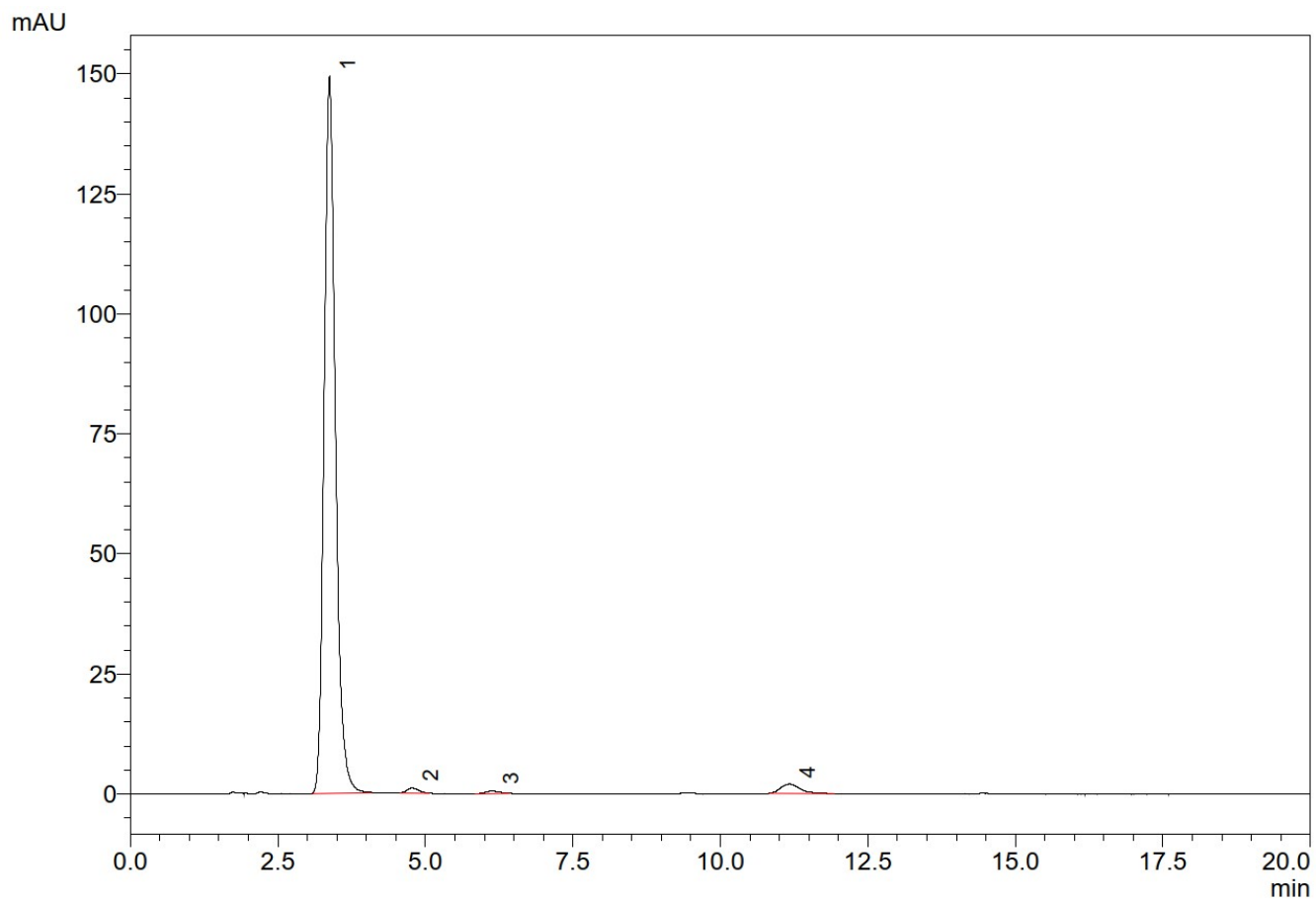


**Figure S 19:** HPLC measurement of an electrolyte containing 0.05 M HMF in 1 M KOH after electrochemical transformation. Assignment of the signals according to the identifiers: FDCA (1), FFCA (2), HMFCA (3), and HMF (4).

## 6. Catalyst characterization

A detailed study of the used catalyst is reported in a previous work.<sup>5</sup> The iron content of the used electrodes was measured by applying ICP-OES. The measurements confirm similar iron loading when compared to the catalyst studied in our previous work.

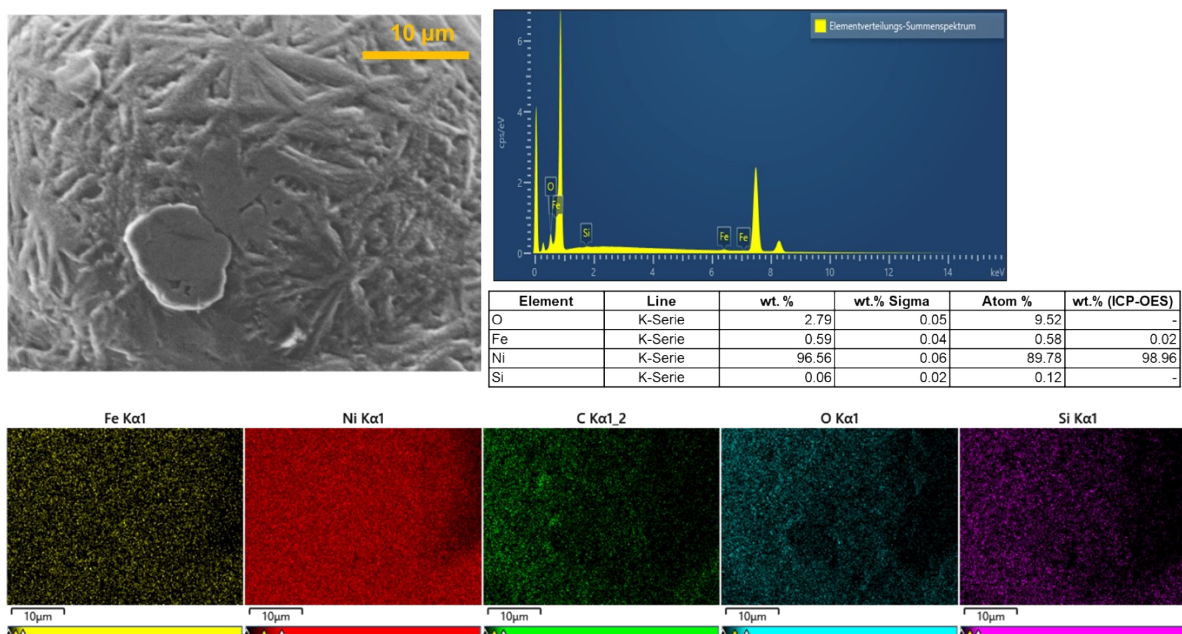


Figure S20: Structural characterization of Fe modified Ni-foams by SEM and ICP-OES analysis.

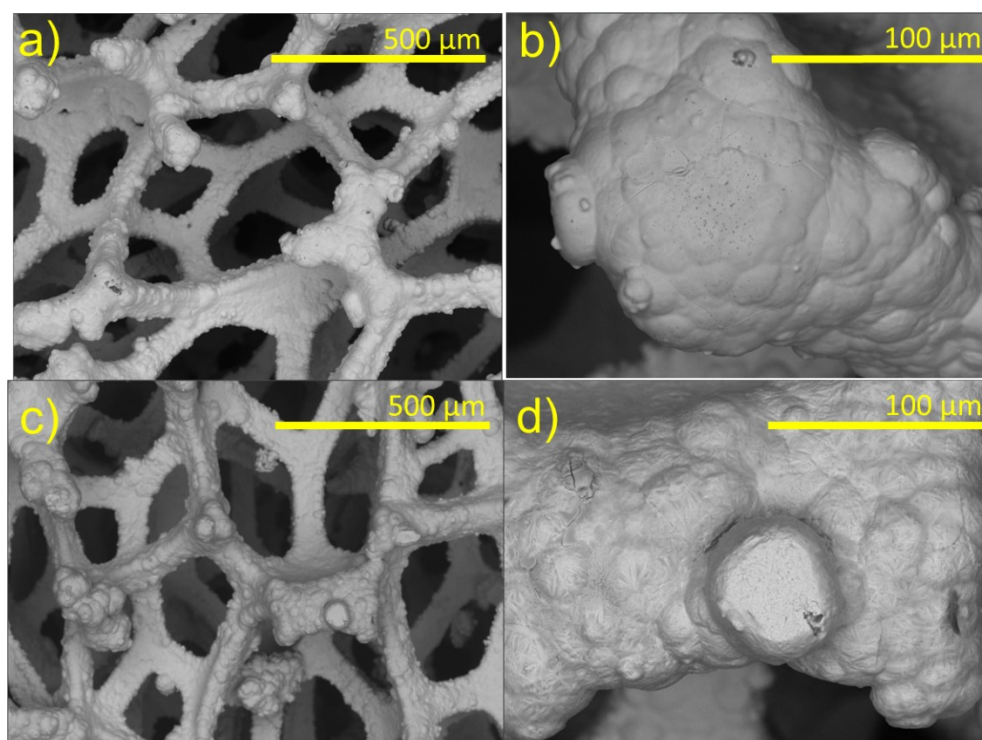


Figure S21: Ni-Foam before (a and b) and after (c and d) Fe modification.

## 7. Testing of indirect HMF oxidation for other catalytic systems

To test whether the pathway of indirect HMF oxidation, meaning the oxidation of the Cannizzaro products DHMF and HMFCa to FDCA, is also possible with different catalytic systems, we test this reaction using mesoporous Cobalt oxide ( $m\text{-Co}_3\text{O}_4$ ) and a Ni-Foam without iron modification.

### 7.1. Unmodified Ni-Foam

Unmodified Ni-Foams were prepared similarly to the Ni(Fe)-electrodes by just skipping the iron modification with  $\text{FeCl}_3$  and  $\text{H}_2\text{O}_2$ . In short, nickel foams were cut into slices (1 cm x 3 cm) and were then cleaned by sonication sequentially using hydrochloric acid (3 M), acetone, ethanol, and ultrapure water for 15 min, respectively. The cleaned foam was then dried at 50 °C for 24 h in air. Electrochemical experiments were performed as described in section 2.3.

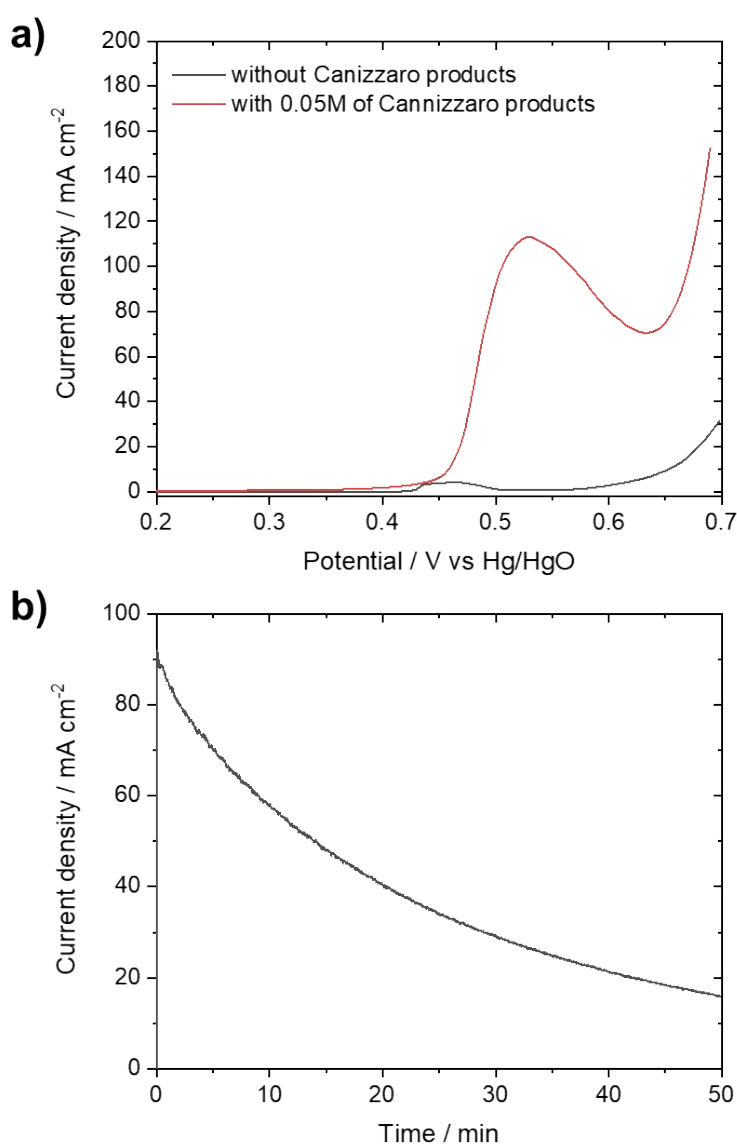


**Figure S22:** Results obtained when testing the Ni-foam electrode. a) LSV measurements in 1M KOH with and without the addition of 0.05 M of the Cannizzaro products (DHMF and HMFCa). Potentials are corrected for the uncompensated solution resistance. b) Constant potential electrolysis at 0.5 V vs. Hg/HgO reference electrode in the presence of 0.05 M Cannizzaro products in 1 M KOH.

LSV measurements (Figure S22a) revealed that by adding the Cannizzaro products to the electrolyte results in a stark increase of the measured currents in the regime for the  $\text{Ni}^{2+}$  to  $\text{Ni}^{3+}$  oxidation at  $\sim 0.45$  V vs. Hg/HgO, similar to the used Ni(Fe)-electrodes. While the increase in currents is not as stark as for the Ni(Fe)-electrodes, these currents are likely to come from the oxidation of the organic substrates. Using constant potential electrolysis (Figure S22b) at 0.50 V vs. Hg/HgO, results in an overall

conversion of 83%, with selectivity and FE of ~99% for the formation of FDCA. A change in the carbon balance was not observed, indicating that the electrolyte was stable against humin formation. Overall, these results demonstrate that commercial Ni-foams can be used to selectively and efficiently oxidize the Cannizzaro products as HMF equivalents in the “indirect” HMF oxidation to FDCA. The oxidation of the Cannizzaro products might therefore be well transferable to other Ni-based electrode materials.

## 7.2. Mesoporous $\text{Co}_3\text{O}_4$

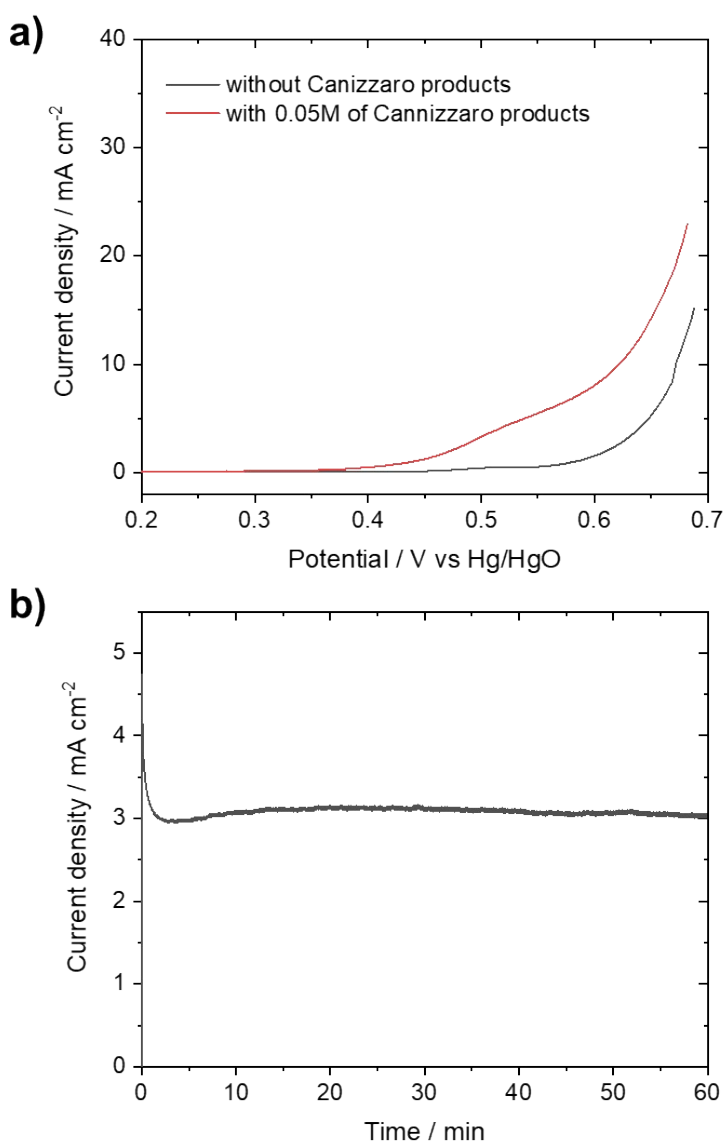


**Figure S23:** Results obtained when testing the  $m\text{-Co}_3\text{O}_4$  catalyst. a) LSV measurements in 1 M KOH with and without the addition of 0.05 M of the Cannizzaro products (DHMF and HMFCFA). Potentials are corrected for the uncompensated solution resistance. b) Constant potential electrolysis at 0.5 V vs. Hg/HgO reference electrode in the presence of 0.05 M Cannizzaro products in 1 M KOH.

$m\text{-Co}_3\text{O}_4$  was prepared by a hard templating method using silica (KIT-6) as the template, followed by impregnation with  $\text{Co}(\text{NO}_3)_2$  and subsequent calcination to the oxide. A detailed description of the synthesis and an in-depth characterization of the catalyst was done in our department and published by Deng *et al.*<sup>6</sup> We recently studied the use of  $m\text{-Co}_3\text{O}_4$  in alkaline HMF oxidation, demonstrating its high efficiency and selectivity in the electrochemical HMF oxidation to FDCA and therefore making it an excellent candidate for performing the oxidation of the Cannizzaro products.<sup>7</sup> To test the performance of the cobalt catalyst, 4.8 mg of the catalyst were mixed with 900  $\mu\text{L}$  of a water/2-propanol mixture (1:3 ratio) and 100  $\mu\text{L}$  of Nafion, followed by sonication for 30 min to obtain a homogeneous

catalyst ink. To prepare the electrode, the catalyst ink was deposited on carbon paper (1 cm x 1 cm; impregnation on both sides) via drop-casting with a target weight loading of 480  $\mu\text{g}/\text{cm}^2$ . The carbon paper was then dried for 24 h at room temperature. Electrochemical experiments were performed as described for the Ni-foam catalysts.

The obtained results for the cobalt catalyst are shown in Figure S23. LSV measurements (Figure S23a) indicate that the addition of the Cannizzaro products, DHMF and HMFCA, result in increased currents in the pre-OER region at potentials < 0.60 V vs. Hg/HgO reference electrode. These currents are likely to originate from the electrochemical oxidation of DHMF and HMFCA towards FDCA. To further study the oxidation process, constant potential electrolysis at 0.50 V vs. Hg/HgO reference electrode was applied (Figure S23b). After 1 h, a conversion of ~5% was determined (Figure S24). FDCA is formed as the main product with a selectivity of ~98% and a FE of ~99%. Compared to the Ni-foam electrodes, the cobalt catalyst shows a much lower conversion. Nonetheless, the result indicates that the efficient and selective oxidation of DHMF and HMFCA is also possible using other electrode designs and materials besides Ni. No change in the carbon balance is observed, demonstrating that the electrolyte was stable against humin formation.

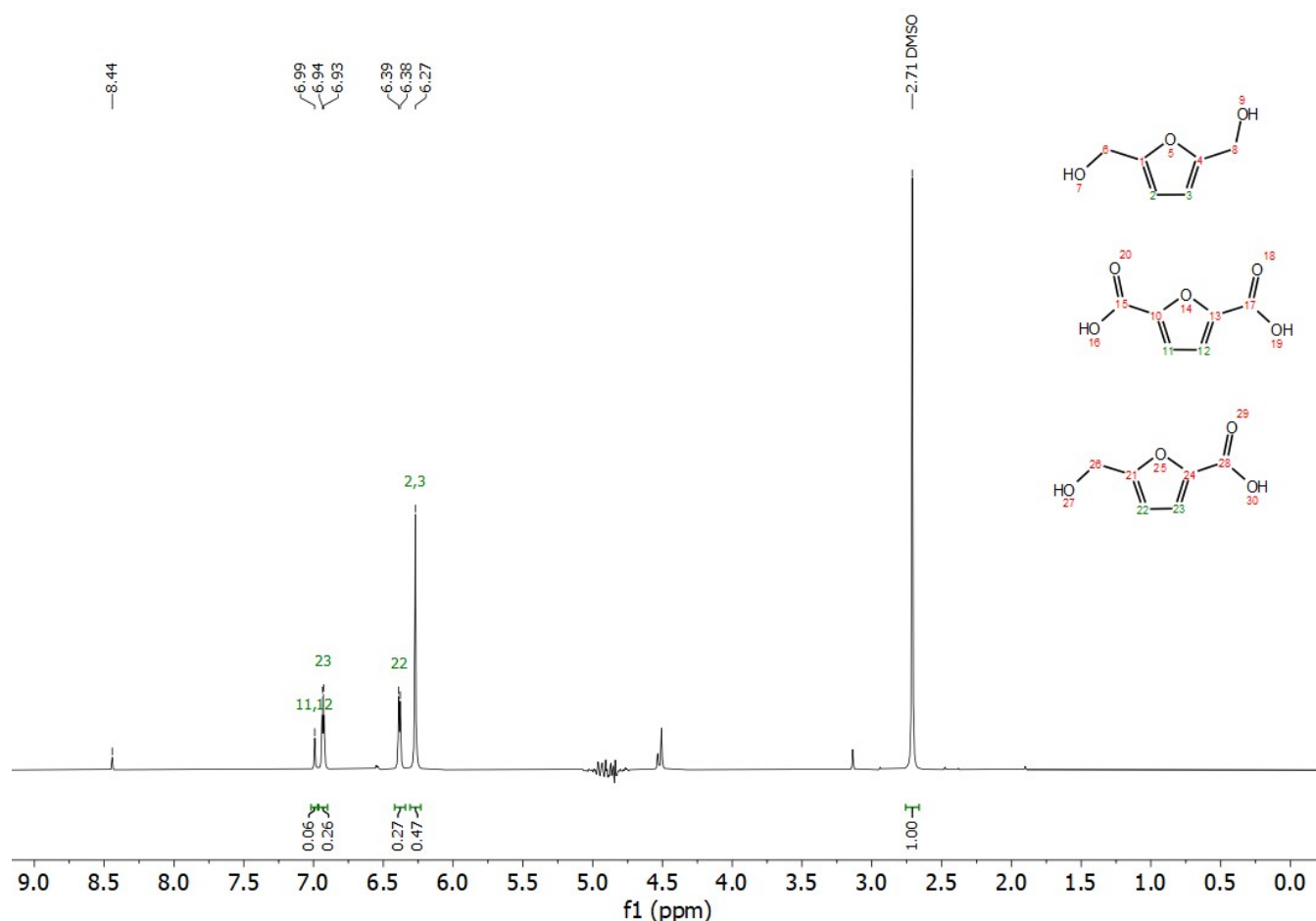


**Figure S24:** qNMR measurement after electrolysis of a 0.05M solution of the Cannizzaro products (DHMF and HMFCA) in 1M KOH using the  $\text{Co}_3\text{O}_4$  catalyst. The sample was diluted with MQ water before the qNMR measurement. Unlabeled hydrogen atoms are affected by the water suppression measurement sequence. Signals at ~ 3.7 ppm and ~ 1.3 ppm are artifacts of the measurement sequence and do not have any analytical relevance. Chemical shifts are referenced by the DMSO signal.<sup>2</sup>

### 7.3. Pt-foil

Noble metals are also known to oxidize HMF to FDCA.<sup>8,9</sup> Therefore we exemplarily studied the oxidation of a mixture of the Cannizzaro products to FDCA (Figure S25) using a Pt-sheet. Electrochemical experiments were performed as described in section 2.3.

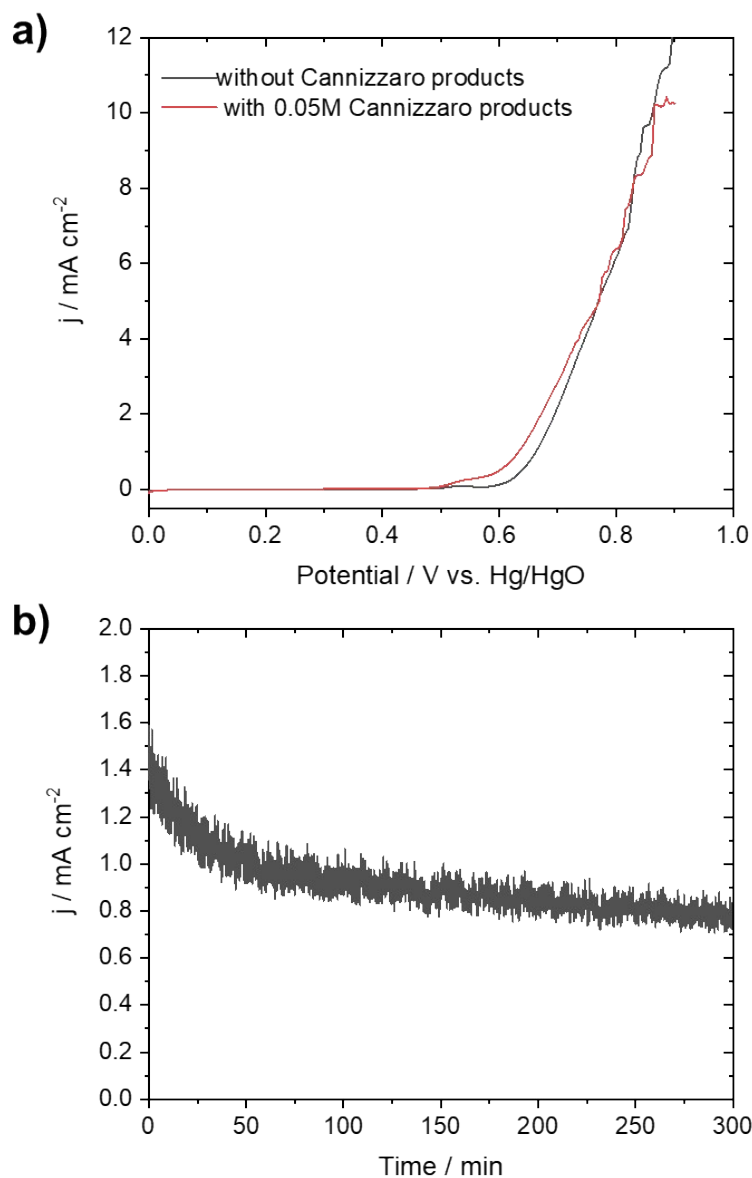


**Figure S25:** Results obtained when using Pt-foil as the catalyst. a) LSV measurements in 1 M KOH with and without the addition of 0.05 M of the Cannizzaro products (DHMF and HMFCa). Potentials are corrected for the uncompensated solution resistance. b) Constant potential electrolysis at 0.7 V vs. Hg/HgO reference electrode in the presence of 0.05 M Cannizzaro products in 1 M KOH.

As demonstrated in Figure S25a, the addition of HMFCa and DHMF does result in a slight increase in currents at potentials of about 0.5 V, indicating electrochemical oxidation. In comparison to the here tested transition metal catalysts, the difference between the two LSVs is relatively small which makes selective conversion of the Cannizzaro products to FDCA more challenging. To study the electrochemical conversion we investigate constant potential electrolysis at 0.7 V vs. Hg/HgO (Figure S25b). After 5h, the formation of 0.3 mM FDCA are detected, which equals less than 1 % conversion while achieving FE of 88 % (Figure S26). Since the concentration of FDCA is close to the detection minimum, it is difficult to yield precise data for the FE. Nonetheless, based on the findings in

Figure S25a, we expect partial contribution of the OER which might explain the comparably low FE. Overall, the results demonstrate that more advanced catalytic systems as well as detailed investigation of the reaction conditions are needed for the oxidation using Pt catalysts. Nonetheless, the results demonstrate that Pt catalysts are expected to oxidize both DHMF and HMFCFA to FDCA when sufficient potentials are applied.

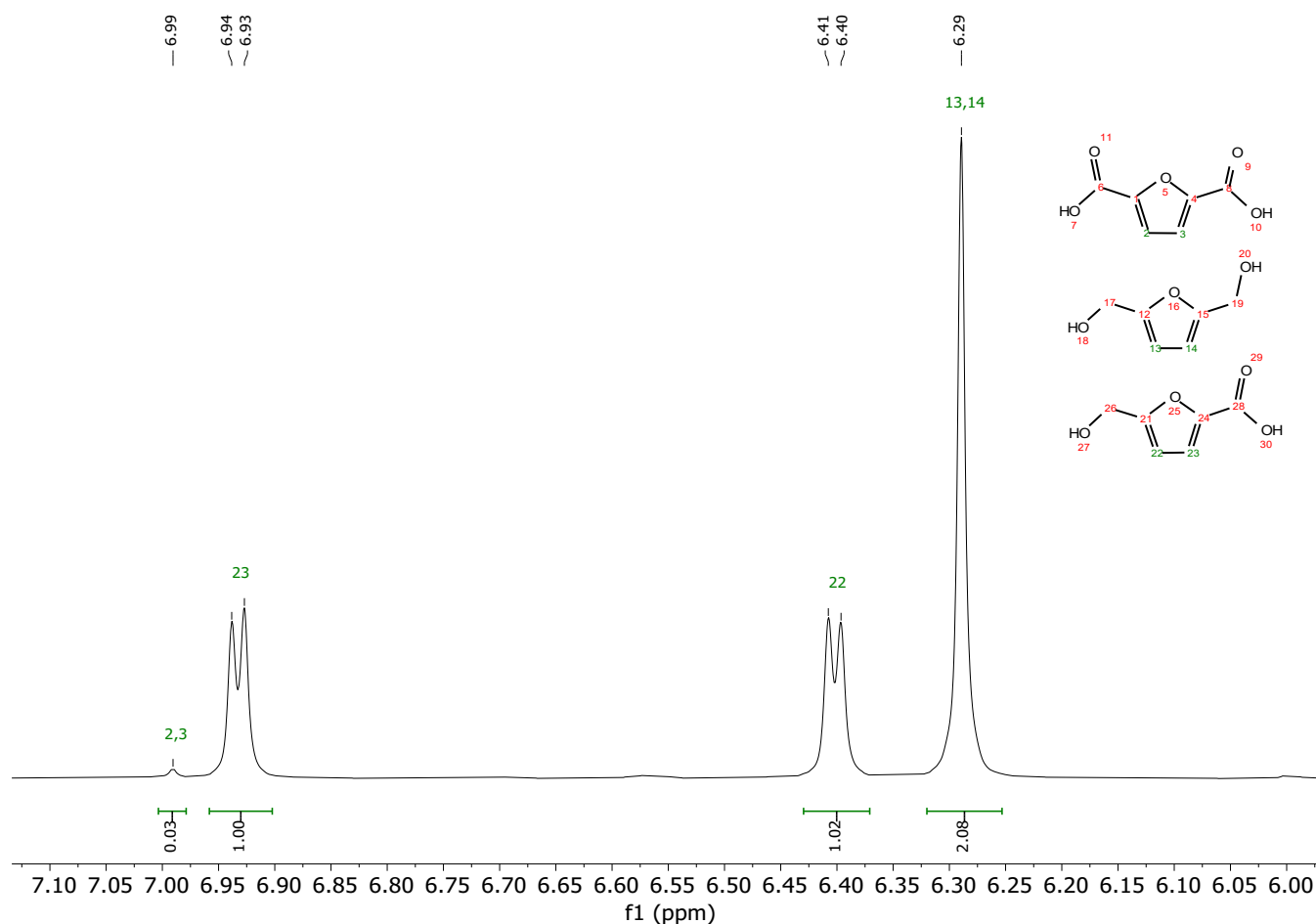


**Figure S26:** qNMR measurement after electrolysis of a 0.05M solution of the Cannizzaro products (DHMF and HMFCFA) in 1M KOH using Pt-foil as the catalyst. The sample was diluted with MQ water before the qNMR measurement. Chemical shifts are referenced by the DMSO signal.<sup>2</sup>

## 8. References

- 1 S. Niu, S. Li, Y. Du, X. Han and P. Xu, *ACS Energy Lett.*, 2020, **5**, 1083–1087.
- 2 N. R. Babij, E. O. McCusker, G. T. Whiteker, B. Canturk, N. Choy, L. C. Creemer, C. V. D. Amicis, N. M. Hewlett, P. L. Johnson, J. A. Knobelsdorf, F. Li, B. A. Lorsbach, B. M. Nugent, S. J. Ryan, M. R. Smith and Q. Yang, *Org. Process Res. Dev.*, 2016, **20**, 661–667.
- 3 T. L. Hwang and A. J. Shaka, *J. Magn. Reson.*, 1995, **112**, 275–279.
- 4 R. W. Adams, C. M. Holroyd, J. A. Aguilar, M. Nilsson and G. A. Morris, *Chem. Commun.*, 2013, **49**, 358–360.
- 5 C. Wang, Y. Wu, A. Bodach, M. L. Krebs, W. Schuhmann and F. Schüth, *Angew. Chem. Int. Ed.*, 2022.
- 6 X. Deng, K. Chen and H. Tüysüz, *Chem. Mater.*, 2017, **29**, 40–52.
- 7 C. Wang, H.-J. Bongard, M. Yu and F. Schüth, *ChemSusChem*, 2021, **14**, 5199–5206.
- 8 H. Xu, X. Li, W. Hu, Z. Yu, H. Zhou, Y. Zhu, L. Lu and C. Si, *ChemSusChem*, 2022, **15**, e202200352.
- 9 D. J. Chadderdon, Le Xin, J. Qi, Y. Qiu, P. Krishna, K. L. More and W. Li, *Green Chem.*, 2014, **16**, 3778–3786.